Energy Fuels **2009,** *23,* 4470–4478 · DOI:10.1021/ef900107b
Published on Web 07/31/2009

energy&fuels
article

Optimization Principle for Variable Viscosity Fluid Flow and Its Application to Heavy Oil Flow Drag Reduction

Qun Chen,[†] Moran Wang,*[,‡] Ning Pan,[§] and Zeng-Yuan Guo[†]

[†]*Key Laboratory for Thermal Science and Power Engineering of Ministry of Education, Department of Engineering Mechanics, Tsinghua University, Beijing 100084, China,* [‡]*Earth and Environmental Sciences Division, Los Alamos National Laboratory, Los Alamos, New Mexico 87545, and* [§]*Department of System Biological Engineering, University of California, Davis, California 95616*

Received February 4, 2009. Revised Manuscript Received July 10, 2009

Drag reduction in heavy oil transport systems is a key for high-efficiency oil transfer and, thus, for energy conservation. In this paper, we investigated the influence of viscosity, velocity, and velocity-gradient fields on drag resistance in fluid flow with variable viscosity in terms of the field synergy. The theoretical analysis indicates that the drag during varying viscosity fluid flow processes depends upon not only the synergy between the velocity and its gradient over the entire flow domain but also the viscosity and velocity gradient at the boundary. That is, for a given flow rate or inlet velocity, simultaneously reducing the fluid flow field synergy number over the entire flow domain and decreasing the fluid viscosity and the velocity gradient at the boundary will lead to a smaller flow resistance. In addition, starting from the basic governing equation and via the calculus of variations, we derived Euler's equation, essentially the momentum equation with a special additional volume force, using the criterion of the minimum viscous dissipation rate to optimize the flow processes for varying viscosity fluid. For fixed flow rate or inlet velocity, solving Euler's equation will result in the optimal velocity and viscosity fields, leading to the minimized flow resistance. Finally, a thermal insulating transport process for heavy oil was taken as a testing case to demonstrate the application of the theory. The results show that generating longitudinal vortexes to enhance the heat-transfer performance of heavy oil will facilitate the flow drag reduction. For instance, when the inlet heavy oil velocity and the external effective heat-transfer coefficient are 0.01 m/s and 2 W m^{-2} K^{-1}, respectively, the total viscous dissipation rate with a certain presence of longitudinal vortexes is decreased by 19% compared to the result without the vortexes.

1. Introduction

Among all of the worldwide energy use, petroleum is by far the most commonly used fuel source. Both the societies and governments have for a long time recognized the crucial importance of maintaining the petroleum supply for not only economic development but also political stability. At present, with existing reservoirs declining, few giant discoveries, and increased demand, heavy oil, in the short term at least, appears to be an available alternative[1] in place of the conventional petroleum. However, because of the high viscosity of the heavy oil, greater than 0.4 Pa s yet sometimes up to dozens or even hundreds Pa s at room temperature, causing high energy dissipation during transportation, improving heavy oil mobility in transportation still remains a key challenge. Both new technologies and novel design principles for heavy oil transportation are been contemplated to ensure efficient delivery.

During the last several decades, a large number of approaches have been developed to reduce convectional fluid flow drag. For external flows, the streamlined body is constructed or the surface roughness is increased to delay the boundary layer separation from a body. For internal flows, some guide plates are inserted in a curved conduit to eliminate the secondary flows to reduce the flow resistance. Other methods include adding drag-reduction additives of low viscosity[2−4] into fluid and designing the riblet surfaces[5−7] to increase the laminar sublayer thickness. However, these technologies are clearly impractical in heavy oil pipelines. Furthermore, most existing technologies only consider the influence of velocity distribution on the flow drag; therefore, they reduce flow drag mainly by varying the velocity field, e.g., dampening the turbulent fluctuations in the near wall region, while the flow in heavy oil pipelines is laminar or only slightly turbulent and the radial velocity distribution is close to the parabolic profile, which is the optimal flow field with the minimum flow resistance if not considering the influence of viscosity on flow drag.[8]

*To whom correspondence should be addressed. E-mail: mwang@lanl.gov.

(1) Chopra, S.; Lines, L. Introduction to this special section: Heavy oil. *Leading Edge* **2008**, *27* (9), 1104–1106.
(2) Achia, B. U.; Thompson, D. W. Structure of turbulent boundary in darg-reducing pipe flow. *J. Fluid Mech.* **1977**, *81* (JUL13), 439–464.
(3) Li, P. W.; Kawaguchi, Y.; Yabe, A. Transitional heat transfer and turbulent characteristics of drag-reducing flow through a contracted channel. *J. Enhanced Heat Transfer* **2001**, *8* (1), 23–40.
(4) White, C. M.; Somandepalli, V. S. R.; Mungal, M. G. In *The Turbulence Structure of Drag-Reduced Boundary Layer Flow*; Springer-Verlag: New York, 2004; pp 62−69.
(5) Gaudet, L. Properties of riblets at supersonic speed. *Appl. Sci. Res.* **1989**, *46* (3), 245–254.
(6) Neumann, D.; Dinkelacker, A. Drag measurements on V-grooved surfaces on a body of revolution in axial flow. *Appl. Sci. Res.* **1991**, *48* (1), 105–114.
(7) Wang, J. J.; Lan, S. L.; Chen, G. Experimental study on the turbulent boundary layer flow over riblets surface. *Fluid Dyn. Res.* **2000**, *27* (4), 217–229.
(8) Batchelor, G. K. *An Introduction to Fluid Dynamics*; Cambridge University Press: Cambridge, U.K., 1967.

Therefore, several more direct heavy oil flow drag reduction methods have been developed, such as heating the oil, blending the heavy oil with light oil, oil-in-water/surfactant emulsification,[9−12] water-lubricated transport,[13] and catalytic cracking,[14,15] and they have successfully cut down the energy consumption during heavy oil transfer processes. However, each method has its own disadvantages. Both heating the oil and blending the heavy oil with light oil incur additional costs; the surfactant applied reduces the quality of the product oil, and the complex catalytic cracking process requires a great deal of investment.

In fact, most studies on flow drag reduction have focused on reducing the viscosity by physical or chemical methods, while the flow drag depends upon not only the fluid viscosity but also the velocity distribution, as clearly indicated in Newton's viscosity law. Additionally, most drag reduction approaches were developed empirically or semi-empirically with no adequate theoretical basis. Therefore, a much better understanding of the nature of the fluid flow phenomenon is imperative before more effective methodologies in fluid flow optimization can be developed.

For a flow process of fluid with constant viscosity and density, Chen et al.[16] introduced the field synergy concept, referred to as the coupling effect between the velocity and the velocity-gradient fields, to highlight the joint influence of velocity and velocity-gradient fields on the drag. In addition, because viscous dissipation is held as a measure for estimating the irreversibility of a flow process, they developed the minimum viscous dissipation principle for the flow resistance minimization. Nevertheless, because the fluid viscosity was maintained constant, regardless of the temperature or species concentration, neither the energy conservation equation nor the species conservation equation was considered in the optimization process, whereas in practical engineering application, there indeed exist a great number of fluid flow processes with varying physical properties, including viscosity, in heavy oil transportation.

The objective of this paper is, hence, to first investigate the major factors involved, such as viscosity and velocity fields, in studying the flow drag and then develop a minimum viscous dissipation principle with changing viscosity in a fluid flow. Then, starting from the basic governing equations, Euler's equation, i.e., optimization equation, will be deduced by the calculus of variations, the principal objective of this paper, and finally, a heavy oil transport process in a pipe covered by thermal insulators is taken as a testing case to be optimized using Euler's equation to verify the validity of the approach.

2. Field Synergy Principle for Flows with Variable Viscosity

The momentum equation for incompressible steady-state Newtonian flow without the volume force is

$$\rho u_j \frac{\partial u_i}{\partial x_j} = -\frac{\partial P}{\partial x_i} + \frac{\partial}{\partial x_j}\left(\mu \frac{\partial u_i}{\partial x_j}\right) \tag{1}$$

Integrating the momentum equation over the entire flow domain Ω and using Green's theorem[16] yields

$$\int\int\int_{\Omega} \rho u_j \frac{\partial u_i}{\partial x_j} \mathrm{d}V = -\int\int\int_{\Omega} \frac{\partial P}{\partial x_i} \mathrm{d}V + \int\int_{\Gamma} \mu \frac{\partial u_i}{\partial x_j} \vec{n} \mathrm{d}S \tag{2}$$

where Γ, V, and S are the boundary, volume, and surface area of the flow domain, respectively, and $\vec{n}$ is the outward normal unit vector. Then, $D = V/S$ is defined as the characteristic length. By introducing the dimensionless variables

$$\overline{u}_i = \frac{u_i}{u_{\mathrm{in}}},\ \overline{u}_j = \frac{u_j}{u_{\mathrm{in}}},\ \nabla \overline{u}_i = \frac{\nabla u_i}{u_{\mathrm{in}}/D},\ \mathrm{d}\overline{V} = \frac{\mathrm{d}V}{V},\ \text{and}\ \mathrm{d}\overline{S} = \frac{\mathrm{d}S}{S} \tag{3}$$

eq 2 is written as

$$-\frac{D}{\rho {u_{\mathrm{in}}}^2}\int\int\int_{\Omega} \frac{\partial P}{\partial x_i} \mathrm{d}\overline{V} = \int\int\int_{\Omega} \overline{u}_j \frac{\partial \overline{u}_i}{\partial x_j} \mathrm{d}\overline{V} + \frac{1}{\rho u_{\mathrm{in}} D}\int\int_{\Gamma} \mu\left(-\frac{\partial \overline{u}_i}{\partial x_j}\vec{n}\right)\mathrm{d}\overline{S} \tag{4}$$

The term on the left side of eq 4 is the dimensionless pressure drop in the x_i direction, denoted as the drag during the flow

$$\Delta \overline{P}_i = -\frac{D}{\rho {u_{\mathrm{in}}}^2}\int\int\int_{\Omega} \frac{\partial P}{\partial x_i} \mathrm{d}\overline{V} \tag{5}$$

The first term on the right side is the integration of the scalar product between the dimensionless velocity and the dimensionless velocity gradient, representing the field synergy between the velocity and its gradient in the entire flow domain, referred to as the flow field synergy number

$$\mathrm{FS}_i = \int\int\int_{\Omega} \overline{u}_j \frac{\partial \overline{u}_i}{\partial x_j} \mathrm{d}\overline{V} = \int\int\int_{\Omega} \overline{U} \nabla \overline{u}_i \mathrm{d}\overline{V} = \int\int\int_{\Omega} |\overline{U}||\nabla \overline{u}_i| \cos \beta_i \mathrm{d}\overline{V} \tag{6}$$

where β_i is the angle between the velocity and the x_i velocity component gradient. A large value of β_i leads to a small FS_i, indicating a weak synergy between the velocity and the gradient and, consequently, a small flow drag. In addition, it is worth noting that the fluid viscosity μ is not involved in eq 6. In other words, the flow field synergy number is not influenced by the fluid viscosity.

(9) Al-Roomi, Y.; George, R.; Elgibaly, A.; Elkamel, A. Use of a novel surfactant for improving the transportability/transportation of heavy/viscous crude oils. *J. Pet. Sci. Eng.* **2004**, *42* (2−4), 235–243.
(10) Hardy, W. A.; Sit, S. P.; Stockwell, A. Heavy-oil-emulsion pipeline tests meet targets. *Oil Gas J.* **1989**, *87* (10), 39–43.
(11) Shigemoto, N.; Al-Maamari, R. S.; Jibril, B. Y.; Hirayama, A.; Sueyoshi, M. Effect of water content and surfactant type on viscosity and stability of emulsified heavy Mukhaizna crude oil. *Energy Fuels* **2007**, *21* (2), 1014–1018.
(12) Storm, D. A.; McKeon, R. J.; McKinzie, H. L.; Redus, C. L. Drag reduction in heavy oil. *J. Energy Resour. Technol.* **1999**, *121* (3), 145–148.
(13) Arney, M. S.; Ribeiro, G. S.; Guevara, E.; Bai, R.; Joseph, D. D. Cement-lined pipes for water lubricated transport of heavy oil. *Int. J. Multiphase Flow* **1996**, *22* (2), 207–221.
(14) Ovalles, C.; Filgueiras, E.; Morales, A.; Scott, C. E.; Gonzalez-Gimenez, F.; Embaid, B. P. Use of a dispersed iron catalyst for upgrading extra-heavy crude oil using methane as source of hydrogen. *Fuel* **2003**, *82* (8), 887–892.
(15) Weissman, J. G.; Kessler, R. V.; Sawicki, R. A.; Belgrave, J. D. M.; Laureshen, C. J.; Mehta, S. A.; Moore, R. G.; Ursenbach, M. G. Down-hole catalytic upgrading of heavy crude oil. *Energy Fuels* **1996**, *10* (4), 883–889.
(16) Chen, Q.; Ren, J. X.; Guo, Z. Y. Fluid flow field synergy principle and its application to drag reduction. *Chin. Sci. Bull.* **2008**, *53* (11), 1768–1772.

The second term on the right-hand side is the total dimensionless boundary viscous force because of the x_i velocity component gradient, determined by both the dynamic viscosity and the velocity gradient at the boundary

$$\bar{\tau}_i = \frac{1}{\rho u_{\text{in}} D}\int\int_{\Gamma}\mu\left(-\frac{\partial \overline{u}_i}{\partial x_j}\vec{n}\right)\mathrm{d}\overline{S} \tag{7}$$

Substituting eqs 5−7 into eq 4 gives

$$\Delta\overline{P}_i = \mathrm{FS}_i + \bar{\tau}_i \tag{8}$$

As shown in eq 8, the flow drag depends upon two factors: one is the synergy between the velocity and its gradient over the entire flow domain, and the other is the viscous force at the boundary. Hence, for a given flow rate, there are several ways to reduce the flow drag, such as (1) reducing the flow field synergy number by enlarging the synergy angle β_i between the velocity and its gradient and (2) decreasing the fluid viscosity μ and/or the velocity gradient at the boundary Γ, i.e., not the entire flow domain.

This field synergy principle presents a novel approach for analyzing flow processes and sets the direction for developing new flow drag reduction technologies. However, this principle is unable to optimize the flow processes, that is, find out an optimal flow field with minimum flow drag, because there is no such mechanism built into it.

3. Minimum Viscous Dissipation Principle

Because of viscosity, a fluid flow is an irreversible process. The irreversibility, i.e., flow drag, stems from the viscous dissipation of mechanical energy during fluid flow. Thus, for a fluid flow process with a given set of constraints, including the continuity equation, the energy conservation equation, and the flow boundary conditions, the optimization objective is to find an optimal velocity and viscosity fields, which lead to the minimum viscous dissipation. Meanwhile, because the influence of the temperature of heavy crude oils on the viscosity is much larger than that on the density, the density is considered to be fixed during a flow process in most cases, while the viscosity is dependent upon the temperature. Thus, for simplicity, herein, all of the physical properties, except for the viscosity, are assumed to be fixed during a flow process and the viscosity is dependent upon the temperature only regardless of the species concentrations. The optimization objective, criterion, constraints, and boundary conditions are summarized as

(1) Optimization objective: the velocity and viscosity fields associated with the minimum flow drag.

(2) Optimization criterion: the minimum dissipation of mechanical energy, expressed in terms of a variation function.

$$\boldsymbol{\delta}\int\int\int_{\Omega}\phi_{\text{m}}\mathrm{d}V = 0 \tag{9}$$

(3) Constraints:

(a) The continuity equation

$$\nabla U = 0 \tag{10}$$

(b) The energy conservation equation

$$\rho c_{\text{p}} U\nabla T = \nabla(\lambda\nabla T) + \phi_{\text{m}} \tag{11}$$

(4) Flow boundary condition: prescribed boundary velocity, written in terms of the variation function as

$$\boldsymbol{\delta}U|_{\text{b}} = 0 \tag{12}$$

The constraints can be removed using the Lagrange multipliers method to construct a function

$$\Pi = \int\int\int_{\Omega}\{\phi_{\text{m}} + A[\nabla(\lambda\nabla T) + \phi_{\text{m}} - \rho c_{\text{p}} U\nabla T] + B\nabla U\}\mathrm{d}V \tag{13}$$

where A and B are Lagrange multipliers, varying with the position, and ϕ_{m} is the viscous dissipation function

$$\phi_{\text{m}} = \mu(T)\left[2\left(\frac{\partial u}{\partial x}\right)^2 + 2\left(\frac{\partial v}{\partial y}\right)^2 + 2\left(\frac{\partial w}{\partial z}\right)^2 + \left(\frac{\partial u}{\partial y} + \frac{\partial v}{\partial x}\right)^2 + \left(\frac{\partial u}{\partial z} + \frac{\partial w}{\partial x}\right)^2 + \left(\frac{\partial v}{\partial z} + \frac{\partial w}{\partial y}\right)^2\right] \tag{14}$$

or in the tensor form

$$\phi_{\text{m}} = \frac{\mu(T)}{2}\left(\frac{\partial u_i}{\partial x_j} + \frac{\partial u_j}{\partial x_i}\right)^2 = 2\mu(T){s_{ij}}^2 \tag{15}$$

where s_{ij} is the strain tensor, corresponding to the velocity gradient. Equation 15 indicates that the viscous dissipation rate is proportional to the square of the strain tensor.

Herein, assume that the fluid viscosity, μ, exhibits an exponent relation to the temperature, T

$$\ln\mu = kT + b \tag{16}$$

where k and b are both constant. When k equals zero, the fluid viscosity, μ, reduces to a constant value.

The variational of eq 13 with respect to the temperature T yields

$$-\rho c_{\text{p}} U\nabla A = \nabla(\lambda\nabla A) + (1+A)k\phi_{\text{m}} \tag{17}$$

The boundary conditions of the variable A include $A_{\text{b}} = 0$ for prescribed boundary temperatures and $(\partial A/\partial n)_{\text{b}} = 0$ for either fixed surface heat flux or a given convection surface condition, including a known convective heat-transfer coefficient, h_0, and a prescribed ambient temperature, T_0.

The variational of eq 13 with respect to the velocity vector U leads to

$$\mu\nabla^2 U + \frac{1}{2(1+A)}\nabla B + \frac{\rho c_{\text{p}} A}{2(1+A)}\nabla T = 0 \tag{18}$$

Thus, there are four unknown variables and four governing equations including eqs 17 and 18, the continuity eq 10, and the energy conservation eq 11; therefore, the unknown variables can be solved for prescribed boundary conditions. Meanwhile, the fluid flow must also satisfy the momentum conservation equation

$$\rho U\nabla U = -\nabla P + \nabla(\mu\nabla U) + F \tag{19}$$

Comparing eqs 18 and 19 gives the following relations

$$B = -2(1+A)P \tag{20}$$

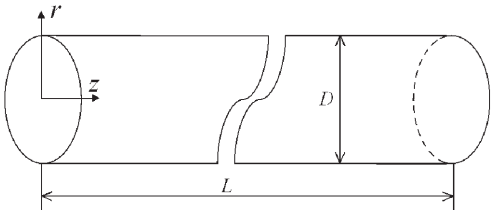

Figure 1. Sketch of the circular pipe.

$$F = \rho U \nabla U - U \nabla \mu + \frac{\rho c_p A}{2(1+A)} \nabla T \quad (21)$$

Substituting eqs 20 and 21 into eq 19 gives

$$\rho U \nabla U = -\nabla P + \nabla(\mu \nabla U) + \rho U \nabla U - U \nabla \mu + \frac{\rho c_p A}{2(1+A)} \nabla T \quad (22)$$

This is Euler's equation, essentially the momentum equation with a special additional volume force defined in eq 21, by which both the velocity and the viscosity fields are adjusted to minimize the viscous dissipation rate, i.e., to optimize the fluid flow. In summary, solving Euler's equation together with eqs 10, 11 and 17 will offer the optimal velocity and viscosity fields, leading to the minimum flow drag at the specific boundary conditions, which give a theoretical basis that would guide the design of heavy oil transportation systems with any density to reduce the flow drag, as long as the density remains constant during the flow process.

4. Drag Reduction for the Heavy Oil Transport Process

4.1. Numerical Model and Method. In engineering, thermal insulating transportation is a usual way to transport hot heavy oil in pipelines. Because the temperature of heavy oil, thus, the oil viscosity, varies along the pipeline because of thermal leakage, the total viscous dissipation during the processes depends upon not only the velocity field but also the temperature distribution over the entire flow path. That is, although the velocity, velocity gradient, and temperature fields all influence the drag during the flow, such a combined scenario is usually not considered in the current pipeline design. Herein, the aforementioned optimization principle will be used in this section to demonstrate its capacity in treating such heated heavy oil transportation problems to hopefully shed some light on the issue.

Consider a heavy oil transport process, for instance, in a circular pipe with diameter, D, = 0.2 m and length, L, = 5 m, as shown in Figure 1. Heavy oil enters the pipe from the left inlet and exits from the right. The inlet average velocity is 0.01 m/s, assumed fully developed, and the inlet and ambient temperatures are 100 and 20 °C, respectively. Here, for the reason of space constraints, the heavy oil is assumed to be a Newtonian fluid and its physical properties include[17−19] $\rho = 950$ kg/m^3, $c_p = 2000$ J kg^{-1} K^{-1}, $\lambda = 0.15$ W m^{-1} K^{-1}, $\mu = e^{-0.085t + 9.6}$ Pa s, all, except the viscosity μ, remaining constant during the flow process, even though the aforementioned optimization principle can also be used for designing any other heavy crude oil transportation systems with any physical parameters. In addition, the viscosity of heavy oil is high enough that the flow in the pipelines is laminar. The optimization objective is to find out a suitable oil velocity distribution to minimize the flow resistance in the pipe at this given flow rate.

The CFD program, FLUENT 6.0, was used to solve the conservation equations together with the corresponding boundary conditions to obtain the fluid velocity and temperature fields in the pipe. The velocity and pressure were linked using the SIMPLEC algorithm, with the convection and diffusion terms discretized using the QUICK scheme. The user-defined function, UDF, in FLUENT is used for solving the govern equations for the parameter, A, and the additional volume forces in eq 22. To save time and memory, only one-fourth of the pipe was mashed and simulated, owing to the symmetry. Figure 2 shows the grid distribution.

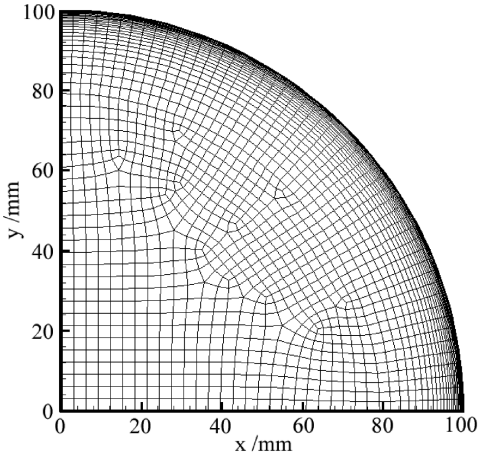

(a) x–y section

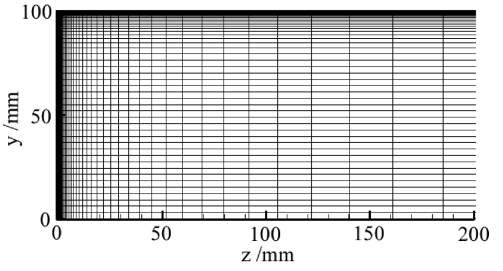

(b) y–z section

Figure 2. Grid distribution of the computation domain.

Table 1. Averaged Flow and Heat-Transfer Parameters of Heavy Oil at the Section of z = 2.5 m for Different Thermal Insulating Boundary Conditions

effective heat-transfer coefficient (W m^{-2} K^{-1})	viscous dissipation rate per volume (W/m^3)	square of the strain tensor (s^{-2})	temperature (°C)	viscosity (Pa s)
0.5	0.26	0.040	99.90	3.15
2.0	0.32	0.044	99.64	3.97

(17) Ali, S. M. F. Heavy oil—Evermore mobile. *J. Pet. Sci. Eng.* **2003**, *37* (1−2), 5–9.
(18) Barrufet, M. A.; Setiadarma, A. Experimental viscosities of heavy oil mixtures up to 450 K and high pressures using a mercury capillary viscometer. *J. Pet. Sci. Eng.* **2003**, *40* (1−2), 17–26.
(19) dos Santos, R. G.; Mohamed, R. S.; Bannwart, A. C.; Loh, W. Contact angle measurements and wetting behavior of inner surfaces of pipelines exposed to heavy crude oil and water. *J. Pet. Sci. Eng.* **2006**, *51* (1−2), 9–16.

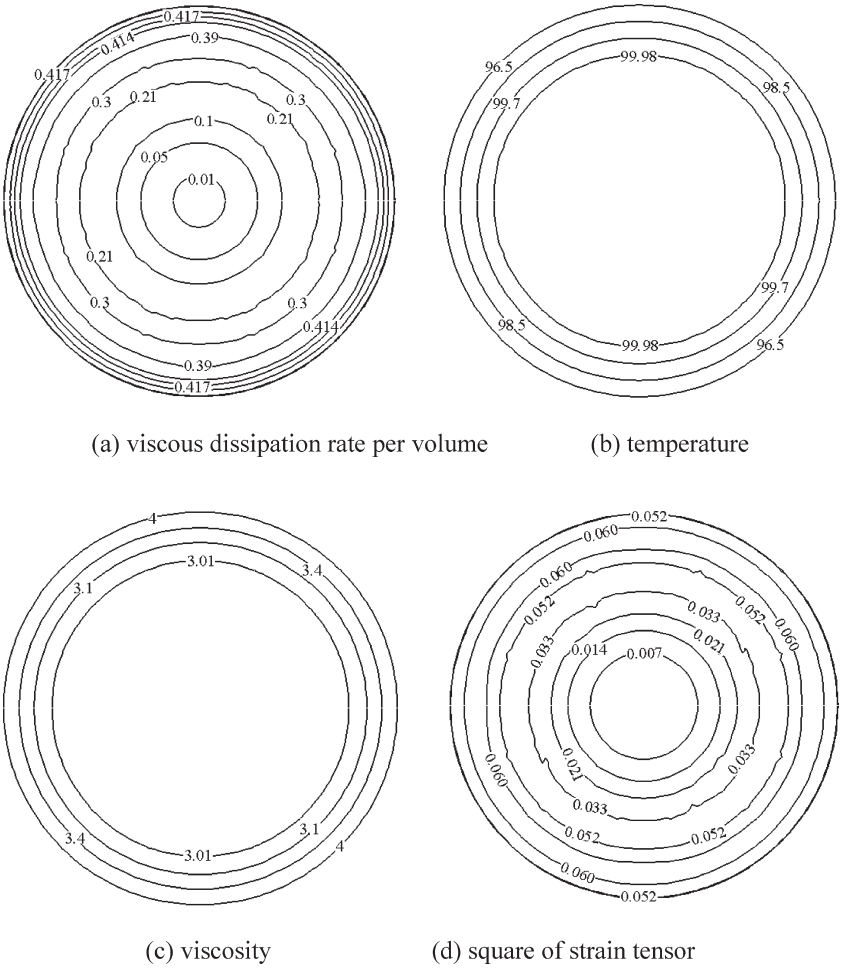

(a) viscous dissipation rate per volume (b) temperature

(c) viscosity (d) square of strain tensor

Figure 3. Original results at the cross-section of $z = 2.5$ m ($h = 0.5$ W m^{-2} K^{-1}).

The mesh is more condense in both the near wall regions and near the inlet, where more steep velocity gradient is expected. The total element of the grid is about 450 000 (1500 grids at the cross-section and 300 grids in the axial direction).

4.2. Results and Discussion. Without any volume force, i.e., $F = 0$ in eq 21, Euler's eq 22 degrades into the original momentum equation with no optimization function. Using the original equation, the average heavy oil flow and heat-transfer parameters at the cross-section of $z = 2.5$ m, under different thermal insulating boundary conditions, are listed in Table 1. When the external effective heat-transfer coefficient, h_o, is 0.5 W m^{-2} K^{-1}, the average values of the viscous dissipation rate per volume, the square of the strain tensor, the temperature, and the viscosity are 0.26 W/m^3, 0.040 s^{-2}, 99.90 °C, and 3.15 Pa s, respectively. Figure 3a is the original distribution of the viscous dissipation rate per volume, indicating that the viscous dissipation rate is greater at the near wall region, about 1.6 times the average value. Figure 3b shows the original temperature distribution. The temperature of the oil in the core annular space approximates to 100 °C, i.e., nearly the inlet temperature, while the temperature at the tube wall is about 95.5 °C, a reduction of 4.5 °C. Because the flow in pipe is laminar, the heat-transfer coefficient is relatively small. When the temperature in the near wall region decreases because of the thermal leakage, the hotter heavy oil in the core annular space cannot transfer the heat to the cooler oil quick enough, resulting in a large temperature decrement of 4.5 °C at the tube wall, even though the average temperature dropped by only 0.1 °C. Furthermore, considering the exponential relationship between them, the viscosity near the wall region is relatively larger.

As shown in Figure 3c, the maximum viscosity is about 1.27 times the average value. In addition, as seen in Figure 3d, the magnitude of the velocity gradient in the near wall region is also greater. From eq 8 of flow drag, a larger viscosity and velocity gradient at the boundary will increase the flow drag or the viscous dissipation rate. In this case, the total viscous dissipation rate, representing the flow drag, in the entire tube during the heavy oil flow process is 4.04×10^{-2} W, while the thermal leakage rate, i.e., heat transferred from the oil to the ambient, is 120.44 W, which means that the averaged outlet temperature is only 0.202 °C lower than the inlet one.

As listed in Table 1, when the external effective heat-transfer coefficient, h_o, is 2.0 W m^{-2} K^{-1}, the predicted average values of the viscous dissipation rate per volume, the square of the strain tensor, the temperature, and the viscosity are 0.32 W/m^3, 0.044 s^{-2}, 99.64 °C, and 3.97 Pa s, respectively. In comparison to the results for the case $h_o = 0.5$ W m^{-2} K^{-1} for the same temperature, the average values of the three parameters are increased by 23, 10, and 26%, respectively. For a fixed flow rate, the average square of strain tensor varies relatively small (10%) at different thermal boundary conditions. Nevertheless, increasing the thermal leakage rate, the average oil temperature, especially the temperature in the near wall region, decreases, resulting in a significant increment of the viscosity

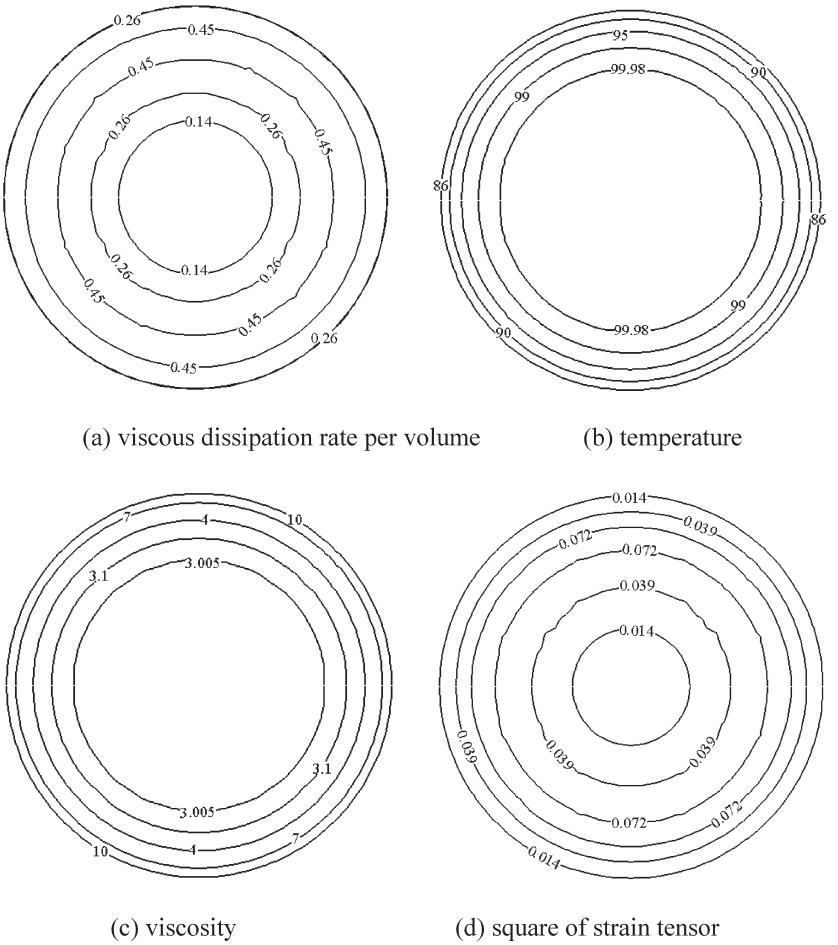

(a) viscous dissipation rate per volume (b) temperature

(c) viscosity (d) square of strain tensor

Figure 4. Original results at the cross-section of $z = 2.5$ m ($h = 2$ W m^{-2} K^{-1}).

there, and consequently, the viscous dissipation rate increases sharply.

For the case of $h_o = 2.0$ W m^{-2} K^{-1}, Figure 4a illustrates the original distribution of the viscous dissipation rate per volume at the cross-section $z = 2.5$ m. The viscous dissipation rate is larger in the region between the tube wall and the center of the pipe but not in the near wall region, different from the results at constant viscosity flow, where the viscous dissipation rate is larger in the near wall region. Figure 4b is the temperature field. Similarly, the oil temperature in the core annular space is close to the inlet temperature, while the temperature at the tube wall is 86 °C, 14 °C lower! Because of the poor heat-transfer performance, the hotter oil in the core annular space cannot transfer heat effectively to the cooler oil, resulting in a large decrement of the temperature in the near wall region, thus a sharp increment of the viscosity, even if the average temperature dropped by only 0.36 °C. As in Figure 4c, the viscosity in the near wall region is about 3 times that in the central area of the pipe. Figure 4d is the distribution of the square of the velocity gradient tensor. The tensor is larger in the region between the wall and the center of the pipe. Because the viscosity of heavy oil is largest near the wall, which hemps the oil flow and decreases the flow velocity, the strain tensor is relatively small, while in the region with some distance from the wall, the viscosity of the oil reduced sharply because of higher temperature, representing a great decrement of the impediment to the flow; therefore, both the velocity gradient and the viscous dissipation rate grow larger than those in any other areas. For this case, the total viscous dissipation rate and thermal leakage in the entire tube during the flow are 5.04×10^{-2} and 417.43 W, respectively. The average outlet temperature is 0.70 °C lower than the inlet one.

In summary, with the absence of the optimization function, because of the thermal leakage/fluctuation and the poor heat-transfer efficiency during the heavy oil insulated transportation process, in the near wall region, the heavy oil is cooler, resulting in an elevated oil viscosity and, consequently, a larger viscous dissipation rate, i.e., a greater flow drag, from eqs 7 and 8.

Now, on the basis of the minimum viscous dissipation principle in Eulier's eq 22 and at $h_o = 0.5$ W m^{-2} K^{-1}, panels a−d of Figure 5 are predicted for the optimized fields, including the cross-section flow, temperature, viscosity, and viscous dissipation rate per volume, at the cross-section of $z = 2.5$ m. As shown in Figure 5a, there exist several longitudinal vortexes in the pipe at the average magnitude of about 2×10^{-4} m/s. Because of these longitudinal vortexes, the oil in the pipe will be forced to mix and have a more uniform temperature; hence, the viscosity, through the cross-section, will be achieved, as shown in panels b and c of Figure 5, compared to the original temperature and viscosity fields in panels b and c of Figure 3, also leading to a reduced viscous force at the boundary. As a result, the flow drag defined in eq 8 during the heavy oil transport process is lowered.

Table 2 compares the heat-transfer parameters of both original and optimized flows during the heavy oil flow. For

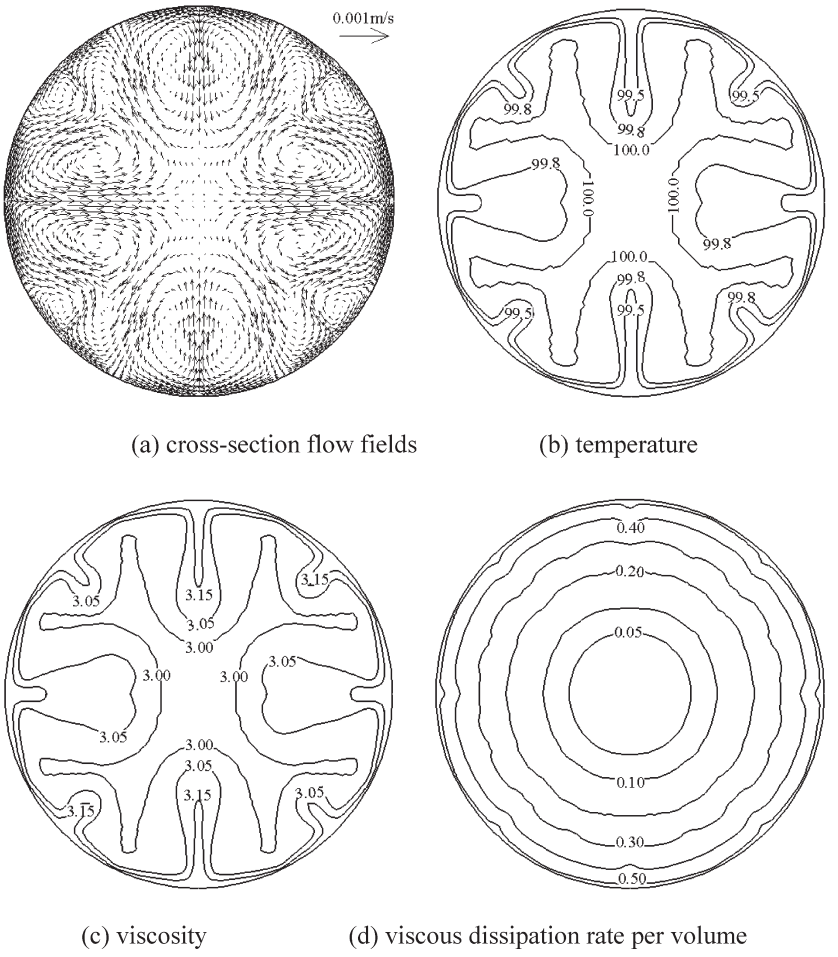

(a) cross-section flow fields (b) temperature

(c) viscosity (d) viscous dissipation rate per volume

Figure 5. Optimized results at the cross-section of $z = 2.5$ m ($h_o = 0.5$ W m^{-2} K^{-1}).

Table 2. Original and Optimized Flow and Heat-Transfer Parameters during Heavy Oil Flow

effective heat-transfer coefficient (W m^{-2} K^{-1})		viscous dissipation rate (W)	outlet temperature decrement (°C)	thermal leakage rate (W)
0.5	original	4.04×10^{-2}	0.202	120.44
	optimized	3.88×10^{-2}	0.208	123.92
2.0	original	5.04×10^{-2}	0.700	417.43
	optimized	4.09×10^{-2}	0.808	482.01

the optimized results with $h_0 = 0.5$ W m^{-2} K^{-1}, the total viscous dissipation rate and thermal leakage in the entire tube are 3.88×10^{-2} and 123.92 W, respectively. The average outlet temperature is 0.208 °C lower than the inlet one. In comparison to the original results with no optimization function, the total thermal leakage rate is increased by 2.9%, while the total viscous dissipation rate, i.e., the drag resistance, is decreased by 4.0%.

If we increase the external heat-transfer coefficient, so that $h_o = 2.0$ W m^{-2} K^{-1}, the corresponding optimized results are shown in Figure 6. In comparison to Figure 5 of $h_o = 0.5$ W m^{-2} K^{-1}, the results are similar. However, the average velocity of the longitudinal vortexes is about 4×10^{-4} m/s, i.e., twice as large as the one in the lower h_o case; the influence from them intensified; and more uniform temperature and viscosity distributions over the cross-section are expected. Because the thermal leakage rate is increased because of a higher external heat-transfer coefficient, the local temperature decrease rate and the local viscous dissipation increase rate of heavy oil in the near wall region are expedited. As listed in Table 2, the total viscous dissipation rate and thermal leakage rate in this case are 4.09×10^{-2} and 482.01 W, respectively. The average outlet temperature is 0.808 °C lower than the inlet one. In comparison to the original results, although the total thermal leakage rate is increased by 15%, i.e., needing more thermal energy, the total viscous dissipation rate during heavy oil flow is decreased by 19%, i.e., consuming less mechanical energy.

In summary, during heavy oil flowing in the pipe, the flow pattern with longitudinal vortexes, to a certain extent, reduces the internal thermal resistance of the convective heat transfer, increases the thermal leakage rate, and enlarges the average viscosity of heavy oil, which overall seem to increase the flow drag. However, because the external thermal resistance is dominative during the heavy oil thermal insulating transport process in a pipe, the reduction of the internal thermal resistance does not significantly increase the total thermal leakage, which means both the average temperature decrement and the average viscosity increment will not be very large. In addition, it is worth noting that generating the longitudinal vortexes leads the central hotter, i.e., low viscosity, oil flowing to the cooler area near tube wall to achieve uniform temperature and viscosity fields, which contributes to dramatically increasing the temperature, i.e., decreasing the viscosity, in the near wall region with larger velocity gradient, and finally, reduces the flow drag from eq 8. Furthermore, when reducing the thermal insulating performance, the strength of the longitudinal vortexes should be

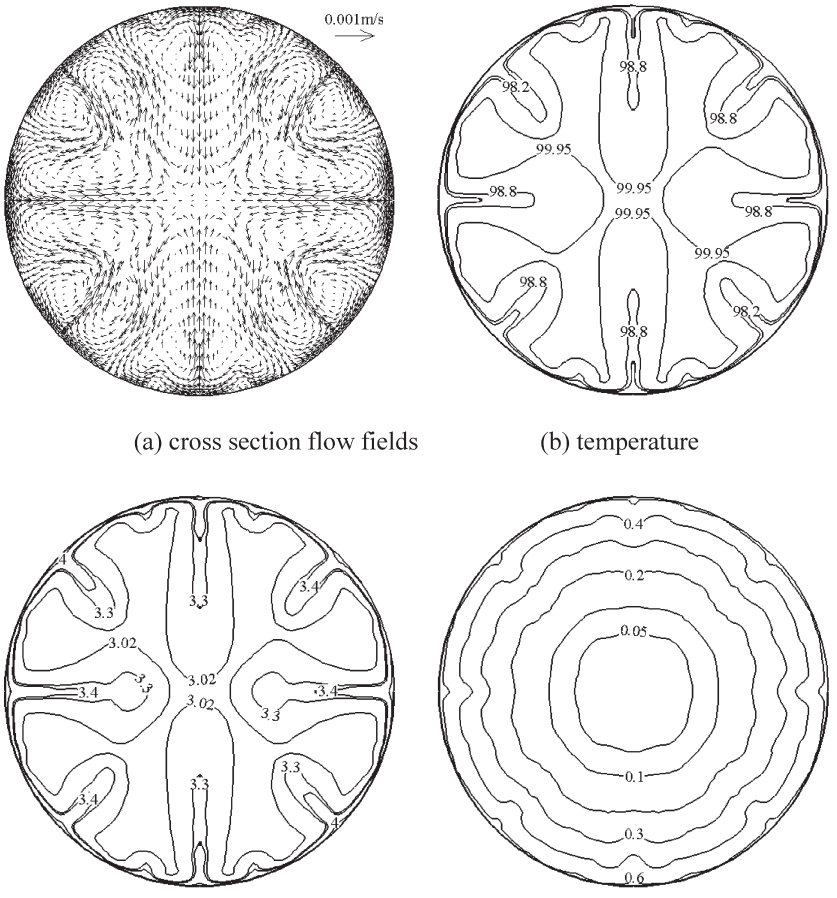

(a) cross section flow fields (b) temperature

(c) viscosity (d) viscous dissipation rate per volume

Figure 6. Optimized results at the cross-section of $z = 2.5$ m ($h_o = 2$ W m^{-2} K^{-1}).

increased to enhance mixing of the central hotter oil and the surrounding cooler oil to obtain uniform temperature and viscosity fields and achieve the objective of drag reduction. In a few words, on the basis of the minimum viscous dissipation principle, the optimal heavy oil flow field, with the minimum flow drag, will be obtained for various thermal insulating conditions.

By the way, using the above optimization principle, we can also discuss the effect of the density on the optimization results, as long as the density remains constant during the flow process, and make some similar conclusions. Most important, derived from the aforementioned discussions, it can be concluded that enhancing the internal heat-transfer efficiency of heavy oil will reduce the flow drag for thermal insulating transport processes. That is to say, not only generating longitudinal vortexes but also some other methods, e.g., adding some high thermal conductivity material including carton nanotubes (CNTs), which does not reduce the quality of product oil, will facilitate the flow drag reduction.

5. Conclusions

Derived from the momentum equation for incompressible steady-state Newtonian fluid without volume force, the influence factors, e.g., the viscosity and velocity fields, of the drag for varying viscosity fluid flows have been investigated in terms of the concept of field synergy. The analysis shows that the flow drag depends upon not only the synergy between the velocity and its gradient over the entire flow domain but also the viscous force at the boundary. For a given flow rate or inlet velocity, the decrease of both the fluid flow field synergy number over the entire flow domain and the fluid viscosity and velocity gradient at the boundary will lead to a smaller flow resistance.

Meanwhile, starting from the basic governing equation and using the calculus of variations, Euler's equation, essentially the momentum equation with a special additional volume force, has been deduced with the criterion of the minimum viscous dissipation rate, as the optimization equation in optimizing varying viscosity fluid flow processes for a given set of constraints. The optimal flow field can be obtained by numerically solving Euler's equation, which leads to the minimum flow drag for a fixed flow rate. This optimal flow field gives a theoretical basis that would guide the design of heavy oil transportation systems with any density to reduce the flow drag, as long as the density remains constant during the flow process.

Finally, a thermal insulating heavy oil transport process in a pipe was taken as a testing case. The velocity, temperature, and viscosity fields in the pipe were optimized on the basis of the minimum viscous dissipation principle. The optimized results show that generating the longitudinal vortexes will lead the central hotter, i.e., low viscosity, heavy oil flowing to the near wall region to sharply decrease the viscosity near the wall with larger velocity gradient and, finally, reduce the flow drag. For instance, when the inlet heavy oil velocity and the external effective heat-transfer coefficient are 0.01 m/s and 2 W m^{-2} K^{-1},

respectively, the total viscous dissipation rate with longitudinal vortexes is decreased by 19% compared to the result without vortexes.

Nomenclature

c_p = specific heat capacity, J kg^{-1} K^{-1}
D = characteristic length, m
F = additional volume force per unit volume, N m^{-3}
$\vec{n}$ = outward normal unit vector
P = pressure, Pa
S = surface area, m^2
T = temperature, K
U = velocity vector
u_i = velocity component in x_i direction, m s^{-1}
u_{in} = inlet velocity, m s^{-1}
V = volume, m^3
ρ = density, kg m^{-3}
μ = dynamic viscosity, kg m^{-1} s^{-1}
λ = thermal conductivity, W m^{-1} K^{-1}
ϕ_m = viscous dissipation rate per unit volume, W m^{-3}
∇ = divergence operator
Π = Lagrange function

Acknowledgment. The present work is supported by the National Key Fundamental R&D Program of China (Grant G2007CB206901).